Magnetic resonance imaging of human tissue-engineered adipose substitutes

Maryse Proulx, MSc,[1,2] Kim Aubin, MSc,[1,2] Jean Lagueux, PhD,[1] Pierre Audet, MSc,[3] Michèle Auger, PhD,[3,4,5] Marc-André Fortin, Ing. PhD,[1,4,6,*] Julie Fradette, PhD,[1,2,*]

[1] Division of Regenerative Medicine, CHU de Québec Research Centre, Québec, G1J 1Z4, G1L 3L5, Canada

[2] Département de Chirurgie and Centre de recherche en organogenèse expérimentale de l'Université Laval / LOEX, Québec, G1J 1Z4, Canada

[3] Département de Chimie, Université Laval, Québec, G1V 0A6, Canada

[4] Centre de Recherche sur les Matériaux Avancés (CERMA), Université Laval, Québec, G1V 0A6, Canada

[5] Regroupement québécois de recherche sur la structure, la fonction et l'ingénierie des protéines (PROTEO), Université Laval, Québec, G1V 0A6, Canada

[6] Département de Génie des Mines, de la Métallurgie et des Matériaux, Université Laval, Québec, G1V 0A6, Canada

∗ **Corresponding authors:** Julie Fradette, PhD and Marc-André Fortin, Ing. PhD. See below for full contact informations.

Submitted to: Tissue Engineering Part C

Keywords: magnetic resonance imaging (MRI), tissue engineering, human adipose tissue, DCE-MRI, self-assembly, volume maintenance

Short title: MRI of tissue-engineered adipose grafts

Authors' contact informations:

Maryse Proulx, MSc

Centre de recherche en organogenèse expérimentale de l'Université Laval / LOEX

CMDGT/LOEX, Aile-R

CRCHU de Québec - Hôpital Enfant-Jésus

1401, 18e Rue, Québec, Qc, G1J 1Z4, Canada

Telephone: 1-418-990-8255 Ext.1671

Fax: 1-418-990-8248

Email: maryse.proulx.2@ulaval.ca

Kim Aubin, MSc

Centre de recherche en organogenèse expérimentale de l'Université Laval / LOEX

CMDGT/LOEX, Aile-R

CRCHU de Québec - Hôpital Enfant-Jésus

1401, 18e Rue, Québec, Qc, G1J 1Z4, Canada

Telephone: 1-418-990-8255 Ext.1717

Fax: 1-418-990-8248

Email: kim.aubin.2@ulaval.ca

Jean Lagueux, PhD

Centre de recherche du CHU de Québec-CHUL

2705 Blv Laurier, Québec, QC, G1V 4G2, Canada

Telephone: 1-418-525-4444 Ext.46140

Centre de recherche du CHU de Québec-SFA

10, rue de l'Espinay, Québec, QC, G1L 3L5, Canada

Telephone: 1-418-525-4444 Ext.53393

Fax: 1-418-525-4372

Email: Jean.Lagueux@crchudequebec.ulaval.ca

Pierre Audet, MSc

Département de chimie

Pavillon Alexandre-Vachon

1045 Avenue de la Médecine, Université Laval, Québec, QC, G1V 0A6, Canada

Telephone: 1-418-656-2131 Ext.4296

Fax: 1-418-656-7916

Email: Pierre.Audet@chm.ulaval.ca

Michèle Auger, PhD

Département de chimie, Faculté des sciences et de génie,

Pavillon Alexandre-Vachon, local 2240 H

1045, Avenue de la Médecine, Université Laval, Québec, QC, G1V 0A6, Canada

Telephone: 1-418-656-3393

Fax: 1-418-656-7916

Email: Michele.Auger@chm.ulaval.ca

Marc-André Fortin, Ing. PhD

Département de génie des mines, de la métallurgie et des matériaux

Pavillon Adrien-Pouliot (bur.1745C); Université Laval, Québec, QC, G1V 0A6, Canada

Telephone: 1-418-656-2131 Ext.8682

Fax: 1-418-656-5343

Email: Marc-Andre.Fortin@gmn.ulaval.ca

Julie Fradette, PhD

Département de chirurgie

Pavillon Ferdinand-Vandry, Université Laval, Québec, QC, G1V 0A6, Canada

CMDGT/LOEX, Aile-R

CRCHU de Québec - Hôpital Enfant-Jésus

1401, 18e Rue, Québec, Qc, G1J 1Z4, Canada

Telephone: 1-418-990-8255 Ext.1713

Fax: 1-418-990-8248

Email: julie.fradette@chg.ulaval.ca

Abstract

Adipose tissue (AT) substitutes are being developed to answer the strong demand in reconstructive surgery. To facilitate the validation of their functional performance *in vivo*, and to avoid resorting to excessive number of animals, it is crucial at this stage to develop biomedical imaging methodologies enabling the follow-up of reconstructed AT substitutes. Until now, biomedical imaging of AT substitutes has scarcely been reported in the literature. Therefore the optimal parameters enabling good resolution, appropriate contrast and graft delineation, as well as blood perfusion validation, must be studied and reported. In this study, human adipose substitutes produced from adipose-derived stem/stromal cells using the self-assembly approach of tissue engineering were implanted into athymic mice. The fate of the reconstructed AT substitutes implanted *in vivo* was successfully followed by magnetic resonance imaging (MRI), which is the imaging modality of choice for visualizing soft ATs. T_1-weighted images allowed clear delineation of the grafts, followed by volume integration. The MR signal of reconstructed AT was studied *in vitro* by proton nuclear magnetic resonance (^{1}H-NMR). This confirmed the presence of a strong triglyceride peak of short longitudinal proton relaxation time (T_1) values (200 ± 53 ms) in reconstructed AT substitutes (total T_1 = 813 ± 76 ms) which establishes a clear signal difference between adjacent muscle, connective tissue and native fat (total T_1 ~ 300 ms). Graft volume retention was followed up to 6 weeks after implantation revealing a gradual resorption rate averaging at 44% of initial substitute's volume. In addition, vascular perfusion measured by dynamic contrast-enhanced (DCE)-MRI confirmed the graft's vascularization post-implantation (14 and 21 days after grafting). Histological analysis of the grafted tissues revealed the persistence of numerous adipocytes without evidence of cysts or tissue necrosis. This study describes the *in vivo* grafting of human adipose substitutes devoid of exogenous matrix

components, and for the first time, the optimal parameters necessary to achieve efficient MRI visualization of grafted tissue-engineered adipose substitutes.

Introduction

Adipose tissue (AT) regeneration is a field of active investigation, encompassing autologous fat grafting, cellular therapies as well as tissue engineering endeavors. Trauma, tumor resection, congenital or acquired anomalies are the main causes justifying the need for adipose substitutes in reconstructive surgery. In 2013 and in the USA only, more than 5.7 million patients have benefited from surgical reconstruction, and 4.4 of them as the result of tumor resection.[1]

Tissue engineering is emerging as a promising alternative to autologous fat transfer for addressing the low predictability of fat transplantation, in particular for breast and facial reconstructive surgical procedures (reviewed in [2, 3]). AT, as a source of adult multipotent stem cells, is now central to many innovations in regenerative medicine.[4-7] Methodologies have been developed to produce tissue-engineered adipose substitutes from different cell sources, including adipose-derived stem/stromal cells (ASCs) (reviewed in [8, 9]).

It is crucial at this stage to develop *in vivo* imaging methodologies enabling the follow-up of reconstructed AT substitutes after implantation.[10, 11] Such procedures are necessary to facilitate the validation of their functional performance *in vivo*, and to avoid resorting to excessive number of animals for each newly developed AT substitute. Until now, biomedical imaging of *in vitro* engineered AT substitutes has scarcely been reported in the literature. Therefore, the optimal parameters enabling good resolution, appropriate contrast and graft delineation, are not clearly established. Invariably, the optimization of tissue visualization in biomedical imaging

necessitates a comprehensive investigation over its physico-chemical characteristics. In magnetic resonance imaging (MRI) for instance, the signal directly depends on the longitudinal and transverse proton relaxation times (namely T_1 and T_2), which are intrinsic to each biological tissue. Differences in signal give rise to contrast effects allowing the delineation of adjacent tissues. In a complementary manner, whether autologous (native) or engineered AT substitutes are implanted, one of the main factors influencing the outcome of graft survival is adequate tissue vascularization.[12-15] Therefore, optimal biomedical imaging methodologies to study the implantation of reconstructed AT must also address the validation of blood perfusion. Overall, such a comprehensive pre-clinical approach will pave the way to the development of future clinical imaging procedures necessary to follow up graft volume retention and functional integration into the surrounding tissues.

Micro-computed tomography (microCT), probably the most widely used imaging modality in tissue engineering, has been used for the evaluation of rodent adiposity [16, 17] as well as for the survival assessment of human fat injected into the scalp of athymic mice.[18] However, microCT does not produce strong differences in contrast between tissues of relatively similar density (e.g. between fat and muscle). In order to reach optimal resolutions, it is often necessary to use long exposure times and therefore high doses of ionizing radiation. This restricts the total number of scans that can be performed during follow-up procedures, before impacting on the animal's health. Although widely available both in small-animal research facilities and in clinical centers, CT does not appear as the modality of choice to monitor and study reconstructed AT substitutes.

MRI is emerging as a comprehensive tool for fat quantification.[19, 20] MRI is already used in the clinics to evaluate the success of autologous fat grafting.[21-23] It has also been reportedly used for

AT quantification using various animal models of obesity, and in particular with tissues containing very strong concentrations of lipids.[24-26] Until now, MRI has been reported twice in the context of *in vivo* adipose engineering preclinical studies but has not been used for the follow-up of AT substitutes reconstructed *in vitro* and featuring lipid-filled adipocytes before implantation. The first study utilized preadipocytes injected into a fibrin matrix that were imaged under 9.4 Tesla MRI to monitor the development of adipose tissue.[27] Another investigation using the rabbit dorsal laminectomy model to follow epidural fat repair mediated by adipogenic-induced rabbit ASCs seeded into porous scaffold over 24 weeks.[28] None of these studies provided a comprehensive MR characterization. The relaxometric properties intrinsic to reconstructed AT substitutes, namely T_1, T_2, and proton NMR spectra are pivotal to acquire optimal MRI images of *in vitro* differentiated and engineered AT grafts.

Compared to CT, MRI can provide high-resolution images without the use of ionizing radiation. It also provides rich contrast effects in lipid-containing tissue, as well as between fat tissue and muscle. Indeed, a large fraction of hydrogen-containing molecules in fat tissues have molecular motions close to the Larmor frequency of hydrogen at clinical magnetic field strengths. This results in short longitudinal relaxation T_1 rates and such tissues usually appear brighter in T_1-weighted (T_1-w.) MR images than muscle, connective tissues and blood. In MRI, the signal is produced by the magnetization of hydrogen protons submitted to a strong magnetic field, followed by excitation using a radiofrequency (RF) pulse precisely tuned to match their Larmor frequency at this specific magnetic field. The MR signal intensity is different from tissue to tissue, being mainly influenced by hydrogen density, as well as T_1 and T_2. In particular, T_1 of fat is one of the shortest *in vivo*, and indicates a very rapid recovery of the magnetization between the successive RF pulses. Available on all clinical and pre-clinical MRI systems, and being

widely used, T_1-w. MR sequences allow to establish clear differences between short-T_1 fatty tissues, and organs and tissues with longer T_1 values. In general, bright native fat can be easily identified and delineated by simple signal thresholding from darker structures. For reconstructed AT however, neither the characteristics T_1 and T_2 nor the specific lipid content are known values. The visualization of reconstructed AT substitutes having lipid contents possibly lower than for native fat tissues, must be performed in parallel with a specific proton T_1 and T_2 study. Only with such values is it possible to reach optimal T_1-w. MRI visualization.

Furthermore, insights into the relaxometric properties of reconstructed AT substitutes could validate the possibility of using the triglyceride peak in proton spectra, as an indicator of reconstructed AT retention once implanted *in vivo*. Indeed, magnetic resonance spectroscopy (MRS), which is the translation of NMR to *in vivo* imaging, yields a precise spectrum of chemical composition within one interrogated voxel. The MRS method relies on chemical shift, or differences in the resonant frequencies of fat and water spins. In fact, ^{1}H-MRS has recently developed into a non-invasive gold standard for determination of hepatic lipids; it is also used for the quantification of intramyocellular lipids as well as for determining the composition of fatty acids in visceral AT depots (e.g. brown and white fat)(reviewed in [29]). Studying the proton relaxation properties of reconstructed AT substitutes at this time of their development would therefore provide crucial information on their physico-chemical properties, which are necessary to establish optimal MRI and MRS follow-up procedures.

In this study, adipocyte-containing substitutes were implanted subcutaneously in athymic mice. The adipose engineering strategy is based on the self-assembly method of tissue engineering which results in the production of functional and entirely natural reconstructed AT substitutes.[30,

[31] Briefly, this model utilizes the properties of ASCs to produce an abundant extracellular matrix after exposure to ascorbic acid during long-term culture. The resulting connective cell sheets can then be superposed to produce thicker connective tissues.[32, 33] If an adipogenic induction step is performed in parallel to matrix stimulation, then the resulting tissue sheets feature functional adipocytes filled with lipids.[32, 34] These reconstructed tissues do not contain synthetic or exogenous biomaterials and their production can be customized for shape and thickness. They can perform β-adrenergic mediated lipolysis and secrete various important adipokines.[32] The implanted reconstructed AT substitutes were visualized and followed-up in T_1-w. MRI to enable volume integration. In parallel, the proton relaxation properties of reconstructed AT substitutes were studied providing useful insights to optimize MRI visualization and to reveal the potential of NMR/MRS in the field of reconstructed AT assessment. T_1-w.-based volume determination was performed over a period of 6 weeks, during which dynamic contrast-enhanced (DCE)-MRI was used to demonstrate the vascularization of the grafted adipose substitutes after implantation. Finally, histological studies established the persistence of numerous adipocytes surrounded by an abundant extracellular matrix in the grafts even though volume resorption/remodeling occurred over time.

Materials and Methods

Production of human reconstructed AT substitutes

ASCs were extracted from lipoaspirated subcutaneous AT of two female donors, after written informed consent (38 year-old, body mass index (BMI) of 29.5; 35 year-old, BMI 21.0). Protocols were approved by the institutional ethical review board of the CHU de Québec Research Center. The extracted cells were seeded at a density of 6.7-8.0 x 10^4 cells/cm^2 for

in vitro expansion and batch cryopreservation after primary culture (passage 0).[32] For the production of adipose substitutes, thawed ASCs were expanded and seeded at passage 3 at a density of 1.70-1.94 x 10^4 cells/cm^2 in 6-well plates for series 1 and 2 (Nunc, Thermo Scientific, Ottawa, ON, Canada) as well as 100 mm Petri dishes (BD Falcon, BD Biosciences, Mississauga, ON, Canada) or Omnitray plates (Nunc) for serie 3. All culture dishes contained a filter-paper anchorage device (Whatman, GE Healthcare, Ottawa, ON, Canada) to facilitate manipulation of the construct.[35] The standard DMEM-Ham's-based culture medium was supplemented with a freshly prepared 50 µg/ml (250 µM) ascorbic acid solution (Sigma-Aldrich, Oakville, ON, Canada) and changed every two-three days, throughout the entire culture period. In order to produce adipocyte-containing cellular sheets, the stromal cultures were induced 7 days after seeding by supplementing the media with a standard adipogenic cocktail.[35] After 3-4 days, induction medium was substituted by adipocyte medium consisting of standard medium supplemented with 100 nM insulin, 0.2 nM T3 and 1 µM dexamethasone only (Sigma). Adipocyte medium was used during the whole culture period following adipogenic induction. For comparative purposes, reconstructed connective tissue sheets devoid of adipocytes were also produced by using the standard medium throughout the culture period.[32] Tissue reconstruction proceeded as a multistep protocol based on adaptations of previously published methods from our group.[32, 33, 35] The adipose substitutes were produced according to two main models based on initial cell seeding into 6-well plates for series 1 and 2 (9.6 cm^2), while serie 3 consisted of a model produced from initially larger culture vessels (57-87 cm^2). For each model, cell sheets were gradually formed into the culture plates and lifted with forceps after 31-43 days. They were superposed in groups of three-five cell sheets. After up to seven days of additional time in culture with ascorbic acid supplementation, superposition or folding of these stacked sheets was repeated sequentially, alternating with an additional six to ten days of culture to ensure sheets cohesion,

until thicker adipose or connective tissues were produced (~1 mm-thick for 16-20 superposed cell sheets). Tissues of 1.41 ± 0.36 cm^2 surface area were used for grafting experiments.

Animal model

Athymic *Nu/Nu* mice (males, 7-8 weeks old, Charles River, Saint-Constant, QC, Canada) were cared for according to protocols approved by the Institution Animal Protection Ethics committee. Tissues were grafted subcutaneously to the flanks of the mice (isoflurane-anaesthetized), onto the muscular bed devoid of *panniculus carnosus* and secured with monofilament Nylon sutures (Ethicon, Johnson & Johnson Medical, Markham, ON, Canada). Two independent experiments were performed for a total of 17 grafted reconstructed AT substitutes (serie 1, n = 5; serie 2, n = 6; serie 3, n = 6). As controls and for imaging optimization, one animal was implanted with reconstructed connective tissue on one flank, and reconstructed AT on the other; one animal with reconstructed AT on one flank and human native AT (37 year-old female donor, BMI of 24.3) on the other; finally, a third animal with human native AT on one flank and murine native AT on the other (Fig. S1). Murine inguinal fat pads were harvested from 6-month aged C3H mice (Charles River). Native AT was harvested a few hours before grafting and samples were used for ^{1}H-NMR. Volume correlations (Fig. S3) were calculated on a total of 12 grafts from two distinct experiments, by comparing the MRI-calculated graft volume to the graft weight (reference AT density = 0.92 g/cm^3).[36]

^{1}H-NMR studies of reconstructed adipose, connective and native adipose tissues

^{1}H-NMR was performed on AT samples (resected human and murine fat as well as reconstructed AT substitutes). Tissues (~40 mg/sample) were carefully rinsed in PBS, which was then absorbed on a dust-free paper (Kimwipes, Kimberly-Clark, Mississauga, ON, Canada). The samples were inserted in 3-mm NMR tubes (Norell Inc, Landisville, NJ, USA) and measured in a EFT-60 FT NMR (Anasazi Instruments, Indianapolis, IN, USA) at a proton frequency of 60 MHz. First, spectra were acquired on static samples with a spectral width of 1500 Hz (25 ppm) with 1024 complex points and 4 scans. To allow the measurement of T_1 on each major peak of the spectra, an inversion-recovery (IR) sequence was used with pulse length of 6 μs for 90^{o} pulses (12 μs for the 180^{o} pulses), with 11 different recovery delays (25, 50, 100, 200, 300, 400, 500, 750, 1000, 2000, 4000 ms). A delay of 10 seconds was used between the scans to avoid any T_1 relaxation effect. To allow the measurement of T_2, a Carr-Purcell-Meiboom-Gill (CPMG) sequence was used, with the following parameters: pulse length 6 μs (12 μs for the 180^{o} pulses); the tau value used in the CPMG experiment was 500 μs; the recycling delay was 10 s, and samples were taken at 2, 4, 8, 16, 32, 64, 128 ms (7 points). Chemical shifts were referenced relative to the peak of water at 4.7 ppm.

T_1-weighted spin-echo and short tau inversion-recovery MR imaging

Immediately after surgery, anaesthetized animals placed on a MRI bed were inserted in a dedicated 3.5-cm RF coil (1 Tesla scanner, ASPECT Imaging, Netanya, Israel). Coronal positioning scans were performed first to center both grafts in the field of view (FOV). Then, axial scans were performed in T_1-w. spin echo 2D, over the entire graft area: FOV: 40 mm; 24 slices; 0.9 mm; 0.1 mm slice gap; dwell time 25 ms; 400 x 320; fα 90^{o}; echo time (TE)/repetition

time (TR): 18/850 ms; 4 exc. (averaged); 19min20s. In order to enhance signal differences between native fat and reconstructed AT substitutes, the TR value was matched with the total T_1 of reconstructed AT substitutes (T_1 ~ 813 ms) measured by ^{1}H-NMR (see Table 1). Finally, STIR axial scans were performed using the following parameters: FOV: 40 mm; 4 slices; 0.9 mm; 0.1 mm slice gap; dwell time 25 ms; 400 x 320; fα 90^o; inversion time TI/TE/TR: 115/9.1/3000; 1 exc.; 16 min. To measure the volume of implants, T_1-w. spin-echo axial images were used, and image analysis was performed with Image J (version 1.48r; Wayne Rasband, National Institutes of Health, Bethesda, USA) by two-four independent evaluators. A 3-D median filter was applied on axial images of each graft, before drawing areas of interest around each implant. Graft volumes were calculated by integrating graft sections, followed by multiplication by slice thickness taking into account the interslice gap (0.1 mm).

DCE-MRI of blood perfusion in reconstructed AT substitutes

Vascularization of AT grafts (tissues of serie 1) was measured after 14 and 21 days using DCE-MRI procedures. Mice were cannulated in the caudal tail vein (30G, winged needle) and connected to a catheter (280 µm ID Intramedic™ Polyethylene Tubing PE-10, 60 cm, total volume: 60 µl) bearing the contrast-media syringe. Then, 100 µl intravascular injections of gadolinium-1,4,7,10-tetraazacyclododecane-*N,N',N'',N'''*-tetraacetic-monoamide-24-cascade-polymer (Gadomer 17, invivoContrast GmbH, Berlin, Germany; 100 µmol/kg, 1.82 mg Gd/injection) were used.[37] Gadomer 17 is a water-soluble dendrimer bearing 24 Gd-DOTA units, and following its injection, signal enhancement in perfused tissues can be used to quantify local blood volume.[38, 39] Pre-injection axial scans were performed (T_1-w. sequence,

FOV: 40 mm; 24 slices; 0.9 mm; 0.1 mm slice gap; dwell time 25 ms; 400 x 320; fα 90°; TE/TR: 18/850 ms; 1 exc., 4:32 min, 2 min inter scan delay). After injection, the same sequence was repeated over a period of 90 minutes. At each time point, areas of interest were drawn over each graft and the S_1/S_0 signal ratio was calculated. The relative blood fraction (f) in vascular grafts was calculated from the experimental S_1/S_0 values measured by DCE-MRI. Vascular volume quantification methodology is available in Supplementary Materials and Methods.

Macroscopic and histological analyses

Macroscopic images of the grafts were taken with an EOS Rebel XSi camera (Canon, Mississauga, ON, Canada) at the time of grafting as well as before excision from the muscular bed after three (serie 1 n = 5; serie 2 n = 2) and six weeks (serie 2 n = 4; serie 3 n = 5). Surface area measurements were performed using ImageJ. Excised grafts were divided into samples used for different analyses. Some were fixed in 3.7 % buffered formalin for 24h and embedded in paraffin. Seven micrometers thick sections were stained with Masson's trichrome to reveal extracellular matrix (blue) and cells (pink). Samples from the AT substitutes at the day of implantation were also processed and stained with Masson's trichrome (serie 3, n = 2). Bright-field images were acquired using an Axio Imager.M2 microscope (Zeiss, Toronto, ON, Canada) equipped with an AxioCam ICc1 camera (Zeiss) and the AxioVision software v4.8.2.0 (Zeiss). Multiple 5x-magnified images were acquired (6 to 20) and merged to enable the reconstruction of the entire tissue sections (Adobe Photoshop CS5 Software, Version 12.0, Adobe Systems Incorporated, San Jose, CA, USA). Adipocyte numbers were determined by manual counts of 4 zones from 5x merged images for a total of 0.57 mm^2 per graft (tissues of serie 3, n = 2-4).

Statistical analysis

Data is presented as mean ± standard deviation. Statistical analysis was performed by one-way analysis of variance (ANOVA) followed by Tukey's post-hoc test ($p < 0.05$, $*p < 0.05$, $***p < 0.001$). Spearman's rank correlation coefficient and r^2 coefficient of determination were calculated for volume correlation analysis between MRI-based and weight-based graft volume determination (Fig. S3). Statistical analysis was performed using GraphPad Prism software Version 5.0 (GraphPad Software, La Jolla, CA, USA).

Results

^{1}H-NMR studies of reconstructed adipose, connective and native adipose tissues

Freshly resected tissues and reconstructed adipose and connective tissue samples analyzed by 60 MHz NMR (1.41 Tesla) produced broad ^{1}H proton peaks (Fig. 1), similar to that obtained in NMR (*in vitro*) and MRS (*in vivo*) for lipid-containing tissues.[40-43] In fact, all NMR spectra of reconstructed AT indicated a significant peak in the range 0.5 – 2.2 ppm, as well as a strong water peak (at 4.7 ppm) corresponding mainly to intracellular water (Fig. 1A). The first peak indicated the strong presence of triglycerides (1.3 ppm for –(C**H**)$_2$-; 1.6 ppm for –CO-C**H**$_2$-C**H**$_2$-; 2.02 pm for -C**H**$_2$-C**H**=C**H**-C**H**$_2$-; 2.24 ppm for –CO-C**H**$_2$-C**H**$_2$-).[41, 44] The shoulder on the main water peak around 5.2-5.3, could be an indication of –C**H**=C**H-** and –C**H**-O-CO- protons in lipid molecules.

Murine fat sample spectra (Fig. 1D) shared strong similarities with that of reconstructed AT (Fig. 1A) in particular regarding the fatty acids peak range (0.5 – 2.2 ppm). The triglyceride peaks in

human and murine fat samples were stronger than for reconstructed AT. Also, the triglyceride/water intensity ratios were 0.37, 3.7 and 0.62, for reconstructed AT, human fat and murine fat samples, respectively. A lower presence of water was found in human fat (Fig. 1C), whereas an equivalent fraction was found in reconstructed AT substitutes and murine fat samples. As expected, the characteristic triglyceride peak was not evidenced in the reconstructed connective tissue spectra (Fig. 1B). However, a strong proton population at 3-4.2 ppm could be attributed to the high content of extracellular matrix (proteoglycans, hyaluronic acid, collagen fibers, fibronectin and laminins), through the presence of amino acids and low molecular weight metabolites (3.78 ppm for a-protons/OOC-C**H**(R)-N**H**-; 3.21 ppm for choline/ $-N^{+}(C\mathbf{H}_3)_3$, and 3.45 for taurine/$\mathbf{H}_3N^{+}$-C$\mathbf{H}_2$-C$\mathbf{H}_2$-$SO_3^{=}$).[45] Such strong spectral differences suggest the possibility to use the triglyceride peak evidenced using MRS, as an indicator of adipose content retention in future reconstructed AT follow-up procedures.

The T_1 and T_2 relaxation times of each biological tissue were measured *in vitro* in order to understand the contrast effects obtained *in vivo*, between native and reconstructed AT. The T_1 and T_2 corresponding to the total proton signal are shown in Table 1, along with the T_1 and T_2 specific to each major proton contribution (peak at 4.7 ppm, and peak at 1.3 ppm). First, a strong difference is observed between the T_1 of reconstructed AT substitutes (total $T_1 = 813 \pm 76$ ms), and the T_1 of native fat (total $T_1 \sim 200 – 300$ ms). This difference indicated the possibility to establish clear tissue contrast and delineation effects between reconstructed AT and the native fat, in each animal. With this result, the repetition time (TR) in T_1-w. MRI scans was set to 850 ms, matching the T_1 of reconstructed AT, and establishing clear differences in contrast between the tissues. In addition, the longitudinal relaxivity of reconstructed connective tissues was found to be the longest. The shortening in total T_1 observed for both native fat and reconstructed AT

substitutes, was attributed to the presence of the triglyceride peak at 1.3 ppm, whose specific T_1 was close to 200 ms in each fat-containing tissue. Therefore, no apparent difference in the T_1 relaxivity of the 1.3 ppm peak was observed in both tissues. With this, it is possible to conclude that the global T_1 measured for both native and reconstructed AT, are mainly guided by their relative fraction of triglyceride-related species (1.3 ppm) versus water (4.7 ppm).

On the other hand, the T_2 of both reconstructed adipose and connective tissues were shorter than for native fat, and this indicates that ^{1}H protons are less mobile in these two tissues. For the 1.3 ppm peak (triglycerides) in particular, the T_2 of reconstructed AT substitutes were shorter than their native counterparts, indicating a difference in the nature of the lipids contributing to the MRI signal. Finally, for reconstructed AT substitutes, a much higher T_1/T_2 ratio (9.3) was found for the water peak (4.7 ppm), compared to the peak associated to the triglycerides (1.3 ppm, ratio: 1.85). Short T_1 and long T_2 are associated to signal enhancement in T_1-w. MRI, and therefore the contribution of the triglyceride peak to enhance the signal intensity in reconstructed AT, is clearly significant.

T_1-weighted spin-echo MR imaging of tissue grafts

As mentioned in the previous section, T_1-w. MRI was performed by setting a TR value in the same range as the T_1 of reconstructed adipose grafts (850 ms). Such scanning condition enabled optimal contrast difference between the native fat and the reconstructed AT substitutes. Grafted AT substitutes were clearly visible on the axial images (Fig. S1A, left). In agreement with the NMR data, native fat implants appeared much brighter in MRI than their reconstructed tissue counterparts (Fig. S1B). This is due essentially to the stronger triglyceride contents in the native

tissues. The contours of both reconstructed AT and native fat implants were clearly delineated on each MR slice, with grafts being sufficiently different than the adjacent muscle. A very good correlation (Spearman r = 0.9107) was found between implant weight and the volumes calculated using MR-images acquired just after implantation (Fig. S3).

In addition, a T_1-w. STIR sequence with signal nulling (TI = 115 ms) was used to evidence the homogeneity of signal nulling in fat grafts. Prior to scanning, the T_1 value measured for the triglyceride peak of AT grafts (Table 1) was used to identify the TI necessary for fat nulling in the STIR sequence (< 200 ms). As expected, because *in vitro* NMR T_1 measurements were performed at 1.41 Tesla, the efficient fat nulling TI appeared shorted at 1 Tesla MRI. The signal from human fat appears bright in T_1-w. MRI images (Fig. S2A, left). This signal was largely eliminated using the fat signal nulling STIR sequence (Fig. S2B, upper left). The signal from native subcutaneous fat was also eliminated (Fig. S2B, arrowheads). This confirms the potential usefulness of STIR sequences in future pre-clinical and clinical studies, in particular in cases were the delineation of adipose grafts from the native fat is difficult to achieve with T_1-w. images only.

Determination of volume resorption kinetics of tissue-engineered adipose grafts

Human tissue-engineered AT substitutes produced *in vitro* were easy to handle and suture (Fig. 2A, B). They featured abundant adipocytes and extracellular matrix components at the time of grafting (Fig. 2C) and were visible through skin after implantation (Fig. 2D). T_1-w. MR images were acquired from the day of grafting up to six weeks after implantation (Fig. 3A-D). The volume of each graft (dotted lines) was determined and compared to its initial volume in order to

calculate the percentage of retention over time (Fig. 3E). The mean initial volume of the three series was 160.2 ± 34.4 mm^3. After three weeks, a mean volume retention of 34.8 % was obtained for the tissues of serie 1 although tissues from series 2 and 3 featured a volume maintenance of 71.9% to 87.0%, respectively. From 3 to 6 weeks after grafting, a slow resorption occurred leading to a final mean volume retention of 35.0 % (serie 2) and 53.6 % (serie 3). Upon harvest, macroscopic images revealed a healthy aspect featuring blood vessels surrounding the grafted tissues after three (Fig. 4A, B) and six weeks (Fig. 4E, F). Interestingly, histological analysis revealed the persistence of numerous adipocytes (rounded void spaces) among an abundant extracellular matrix (blue) after both three (Fig. 4C-D) and six weeks (Fig. 4G-H). A rather stable number of adipocytes were quantified from the day of grafting (1000 ± 188 per mm^2) compared to 6 weeks post-grafting (951 ± 105 per mm^2). Capillary-like structures indicative of vascularization were also observed at both time points (Fig. 4C', C'', G'', arrowheads and boxed areas). Finally, while some areas contained more matrix and less adipocytes, no evidence of cyst formation or tissue necrosis were noticeable on the tissue sections analyzed.

Vascular volume quantification in reconstructed adipose tissues by DCE-MRI

The presence of vascularization in AT grafts was assessed by DCE-MRI at day 14 and 21 following graft implantation. During the procedure, a blood-pool paramagnetic contrast agent was injected i.v., and the resulting MR signal enhancement in T_1-w. images, quantified. Representative MR slices used to monitor the signal enhancement in reconstructed AT grafts (serie 1), and which served in blood volume fraction calculations using Equation 6

(Supplementary Materials and Methods), are shown in Fig. 5A, B. The signal enhancement measured for each graft (2 animals, 2 grafts each, n = 4 grafts), was averaged at each acquisition time, and plotted in Fig. 5C (day 14) and 5D (day 21). For all grafts, a strong signal enhancement was evident from the first scan following injection, with a plateau occurring at 15 – 35 min (Fig. 5C, D). An average maximal signal enhancement factor of 1.36 ± 0.05 and 1.31 ± 0.07 was measured at 14 and 21 days in reconstructed AT substitutes after injection of the blood-pool contrast agent (Table 2). The corresponding blood volume fractions (f) were 7.8 ± 1.8 % (at day 14) and 6.2 ± 2.1 % (at day 21)(Table 2).

Discussion

The increasing need of autologous adipose substitutes in reconstructive and cosmetic surgery has prompted the development of various strategies for AT engineering.[8, 46] The tissue engineering approach we used in this study is based on cell sheet engineering that can be customized to produce adipose substitutes of different sizes and shapes that are easily manipulated and sutured.[35] In this model, cultured ASCs produce their own extracellular matrix elements leading to cell sheets that are combined to form thicker human substitutes devoid of exogenous or synthetic biomaterials. Substitutes featuring large surface areas and ~1 mm in thickness were produced (160 mm^3) and grafted to the flanks of athymic mice.

Because it provides in-depth anatomical images without the use of ionizing radiation, and because lipid-containing tissues usually appear bright in T_1-w. MRI, this modality is by far the most advantageous imaging technique to study the implantation of AT grafts *in vivo*. The present

study is the first to demonstrate the possibilities offered by MRI as a non-invasive imaging tool to follow up *in vitro*-engineered human AT substitutes implanted into small animals. In order to reproduce the exact contrast-enhancement effects that would be seen in clinical equipment, we used a 1 Tesla MRI system. These studies were coupled to *in vitro* ^{1}H-NMR measurements of freshly extracted samples, performed at a similar magnetic field strength, at 60 MHz (1.41 Tesla): the strong triglyceride peak present in reconstructed AT substitutes could be advantageously used in the future to validate the retention of AT properties using MRS follow-up procedures.

In the present study, the reconstructed AT substitutes appeared clearly delineated in T_1-w. MRI images. In addition, a very good correlation was found between implant weight and the volumes calculated using MR-images acquired just after implantation (Spearman r = 0.9107). This demonstrates the precision of MRI to repeatedly measure the volume of subcutaneously-implanted adipose grafts over weeks, by opposition to methodologies relying on terminal biopsies. In parallel with volume retention studies, tissue integrity must also be evaluated through histology. Volume determination over 6 weeks using T_1-w. images revealed overall very good tissue maintenance during the first two weeks after grafting. Then, tissue resorption slowly occurred. Among the grafted tissues, we could not associate the observed variability to any specific parameter (graft experiment, type of reconstruction, cell population used, etc.). Three weeks after implantation, some grafted tissues maintained 79.5% of their initial volume (series 2 and 3) while a mean volume retention of 34.8% was measured for others (serie 1). Despite their smaller volume, when grafts samples from these tissues (serie 1) were harvested and analyzed, abundant adipocytes could be observed in absence of oil cysts or tissue fibrosis.

To further enhance the delineation between endogenous native fat and reconstructed AT substitutes, fat signal nulling was used as a proof of concept. In fact, fat nulling sequences such as STIR are widely used in a variety of clinical MR imaging protocols to attenuate the contributions and artifacts specific to highly lipidic tissues and interfaces.[47] Because a large fraction of the signal was intrinsically attenuated by the STIR sequence, fat-nulled images acquired at 1 Tesla in small mice had relatively poor signal-to-noise ratios which could be improved by longer scanning times (Fig. S2B). These images however demonstrate that STIR sequences could be used as a complement to T_1-w. MR imaging to distinguish between endogenous native fat and implanted AT grafts. For larger animals or patients, a larger pool of hydrogen would contribute to the overall signal, therefore leading to better signal-to-noise ratios than on such small 20-gram mice.

As previously mentioned, coupling MRI to MRS would provide a very powerful tool to study, follow up and assess the retention and integrity of the reconstructed AT after *in vivo* implantation. In non-invasive MRS procedures, the spectral signature and intensity of the triglyceride peak could be exploited as an indicator of tissue integrity. Indeed, MRS allows the spatial mapping of spectroscopic differentiation between brown and white fat, between fat and connective tissue and the characterization of liver fat.[19, 29, 41, 44] The present *in vitro* NMR measurements suggest that MRS acquisitions could become crucial assessments to validate the success of reconstructive surgery based on the implantation of engineered tissues. In MRS, each voxel contains the ^{1}H spectroscopic signature of the tissue. In small voxels (< 1 mm^3), acquiring a sufficient amount of signal to distinguish between the peaks is sometimes challenging. In future clinical applications however, large volumes will be implanted. The possibility to rely on slightly larger voxels will translate into much better signal-to-noise ratios in MRS acquisitions. The

potential of MRS relies not that much in the possibility to delineate the contours of grafts, but rather on the possibility to acquire a mapping of the relative contents of triglycerides (i.e. peak at 1.3 ppm). This application does not require as optimal resolutions as for the T_1-weighted delineation scans.

Vascularization of the implanted AT substitutes is a key factor in their survival and long-term volume retention. In the present study, blood vessels were identified among matrix and adipocytes, indicating a degree of vascularization which was further confirmed by DCE-MRI at day 14 and 21. DCE-MRI procedures provide quantitative values of the perfused microvascular volume in tissues [48-50] and this is the first time DCE-MRI is used to validate the perfusion of reconstructed AT substitutes implanted *in vivo*. The use of a blood-pool MRI contrast agent such as Gadomer 17, allows to perform perfusion studies with a contrast agent that is not susceptible to fast extravasation. The corresponding blood volume fractions measured in AT substitutes point to relatively smaller values than the blood volume fractions measured in xenograft tumors in previously reported DCE-MRI studies.[51, 52] However, one should indeed compare DCE-MRI experiments with other measurements of blood perfusion/volume performed in AT but such data are scarce. Laser Doppler flowmeter, ^{133}Xe clearance, ^{103}Ru-labeled microspheres and ^{46}Sc-labeled microspheres have been used to measure blood flow to brown AT.[53, 54] A more recent study reported the use of molecules fluorescing in the near-infrared region to assess blood perfusion in murine brown AT, demonstrating the possibility to perform non-invasive measurements of changes in blood flow and perfusion occurring in a given AT area.[55] To enable the measurement of total blood fraction, it is preferable to use an imaging probe that remains in the blood for prolonged times ("blood pool" contrast agent). The present study demonstrates the

measurement of the total blood volume in AT after the injection of a MRI contrast agent, followed by DCE analysis. All reconstructed adipose grafts were well vascularized by 14 days, and therefore, it is possible to conclude that DCE-MRI can be used to validate the blood perfusion of reconstructed adipose grafts after implantation *in vivo*.

A limited number of studies have been using imaging tools (ultrasounds, CT, MRI) to complement traditional weight/volumetric measurements of *in vitro* or *in vivo* engineered tissues in preclinical studies.[27, 28, 56, 57] However, volume assessment following imaging has been performed for native adipose grafts implanted in combination or not with cells or hydrogels.[18, 58-60] For example, an ultrasonic study of inguinal adipose grafts inserted into the paraspinal area has been performed in Sprague-Dawley rats with 95.9%, 66.3% and 53.4% remaining volume at respectively 30, 60 and 90 days after implantation.[58] CT determination of human native fat grafted to mice skull revealed 62.2% and 60.9% volume maintenance after 8 and 12 weeks, respectively.[18] Among the lowest resorption rates observed, human fat injections (2 ml) into the dorsum of nude mice resulted into 82% volume persistence after 8 weeks as determined by traditional volumetric analysis.[61] In the field of *in vitro* adipose engineering, direct comparison among models is complicated by the variety of biomaterials and animal models used in addition to parameters such as the substitute's initial volume, graft site and choice of method for the evaluation of volume maintenance after grafting. For example, engineered constructs made of ASCs seeded on collagen microcarriers, submitted to adipogenic differentiation and enriched or not in endothelial cells and fibrin matrix grafted to SCID mice featured a weight maintenance at 4 weeks in the range of 10 to 37 % of the volume measured at day 12.[62] Another study has determined a 34-43% weight maintenance at 6 weeks of injected adipocytes combined with chitosan nanospheres loaded with VEGF aiming to promote vascularization through growth

factor release.[63] Importantly, in the present study, although a global decrease from 79.5% to 44.3 % of the initial adipose graft volume occurred between 3 and 6 weeks, an excellent persistence of adipocytes was observed, as well as abundant extracellular matrix and the absence of oil cysts or areas of necrosis. In some occasions when the engineered substitutes were grafted closer to the inguinal fat pad, murine AT development was noted (not shown). Finally, it would be interesting in future studies to investigate if volume stabilization could be achieved at later time-points and if graft preconditioning or co-treatment with various factors could contribute to volume maintenance as was seen for SDF-1α injection.[64]

Conclusion

In vivo implantation of voluminous reconstructed AT substitutes requires the development of imaging procedures addressing volume retention, relaxometric characteristics, and blood perfusion *in situ*, as indicators of graft viability. The present study reports the *in vivo* murine implantation of engineered human AT grafts. A non-invasive assessment of their volume maintenance and perfusion after grafting was performed by MRI. The proton relaxometric characteristics of reconstructed AT substitutes was also measured by ^{1}H-NMR, which provided crucial information necessary to optimize T_1-w. imaging procedures (contrast and delineation between adipose tissues). It also demonstrated that the triglyceride peak could be used to follow-up the integrity of reconstructed AT in future MRS procedures.

Acknowledgements

This study was financed by the Canadian Institutes of Health Research (CIHR grants #84368, #111233 to J. Fradette) as well as by Discovery grants from the National Science and Engineering Research Council of Canada (NSERC, M.A. Fortin (grant #355524-2012), M. Auger

(grant #184177)). Both J. Fradette and M.A. Fortin are grateful to Fonds de la recherche du Québec - Santé (FRQS) for Junior 2 Career Awards. M. Proulx received scholarships from NSERC, FRQS and Canadian Federation of University Women (CFUW). K. Aubin obtained a Fonds de la recherche du Québec – Nature et technologies (FRQNT) graduate scholarship. We acknowledge the support of the Centre de recherche du CHU de Québec du FRQS and of the Réseau ThéCell du FRQS. The authors would also like to acknowledge the valuable contribution of Arnaud Gais, Pascal Morissette Martin, Anne-Marie Moisan, Émilie Chouinard and Mélissa Guignard for their assistance in animal experiments, as well as Drs Félix-André Têtu and Alphonse Roy for providing human tissue samples.

Author Disclosure Statement

No competing financial interests exist.

References

1. American Society of Plastic Surgeons. 2013 Plastic surgery statistics report. Online. Available from: http://www.plasticsurgery.org/news/plastic-surgery-statistics/2013.html. [Accessed March 2014].

2. Patrick, C.W., Jr. Adipose tissue engineering: the future of breast and soft tissue reconstruction following tumor resection. Semin Surg Oncol **19**, 302, 2000.

3. Hsu, V.M., Stransky, C.A., Bucky, L.P., and Percec, I. Fat grafting's past, present, and future: why adipose tissue is emerging as a critical link to the advancement of regenerative medicine. Aesthet Surg J **32**, 892, 2012.

4. Zuk, P.A., Zhu, M., Mizuno, H., Huang, J., Futrell, J.W., Katz, A.J., Benhaim, P., Lorenz, H.P., and Hedrick, M.H. Multilineage cells from human adipose tissue: implications for cell-based therapies. Tissue Eng **7**, 211, 2001.

5. De Ugarte, D.A., Alfonso, Z., Zuk, P.A., Elbarbary, A., Zhu, M., Ashjian, P., Benhaim, P., Hedrick, M.H., and Fraser, J.K. Differential expression of stem cell mobilization-associated molecules on multi-lineage cells from adipose tissue and bone marrow. Immunol Lett **89**, 267, 2003.

6. Gomillion, C.T., and Burg, K.J. Stem cells and adipose tissue engineering. Biomaterials **27**, 6052, 2006.

7. Gimble, J.M., Katz, A.J., and Bunnell, B.A. Adipose-derived stem cells for regenerative medicine. Circ Res **100**, 1249, 2007.

8. Bauer-Kreisel, P., Goepferich, A., and Blunk, T. Cell-delivery therapeutics for adipose tissue regeneration. Adv Drug Deliv Rev **62**, 798, 2010.

9. Philips, B.J., Marra, K.G., and Rubin, J.P. Adipose stem cell-based soft tissue regeneration. Expert Opin Biol Ther **12**, 155, 2012.

10. Xu, H., Othman, S.F., and Magin, R.L. Monitoring tissue engineering using magnetic resonance imaging. J Biosci Bioeng **106**, 515, 2008.

11. Nam, S.Y., Ricles, L.M., Suggs, L.J., and Emelianov, S.Y. Imaging Strategies for Tissue Engineering Applications. Tissue Eng Part B Rev 2014.

12. Kannan, R.Y., Salacinski, H.J., Sales, K., Butler, P., and Seifalian, A.M. The roles of tissue engineering and vascularisation in the development of micro-vascular networks: a review. Biomaterials **26**, 1857, 2005.

13. Laschke, M.W., Harder, Y., Amon, M., Martin, I., Farhadi, J., Ring, A., Torio-Padron, N., Schramm, R., Rucker, M., Junker, D., Haufel, J.M., Carvalho, C., Heberer, M., Germann, G.,

Vollmar, B., and Menger, M.D. Angiogenesis in tissue engineering: breathing life into constructed tissue substitutes. Tissue Eng **12**, 2093, 2006.

14. Nishimura, T., Hashimoto, H., Nakanishi, I., and Furukawa, M. Microvascular angiogenesis and apoptosis in the survival of free fat grafts. Laryngoscope **110**, 1333, 2000.

15. Yamaguchi, M., Matsumoto, F., Bujo, H., Shibasaki, M., Takahashi, K., Yoshimoto, S., Ichinose, M., and Saito, Y. Revascularization determines volume retention and gene expression by fat grafts in mice. Exp Biol Med (Maywood) **230**, 742, 2005.

16. Luu, Y.K., Lublinsky, S., Ozcivici, E., Capilla, E., Pessin, J.E., Rubin, C.T., and Judex, S. In vivo quantification of subcutaneous and visceral adiposity by micro-computed tomography in a small animal model. Med Eng Phys **31**, 34, 2009.

17. Rubin, C.T., Capilla, E., Luu, Y.K., Busa, B., Crawford, H., Nolan, D.J., Mittal, V., Rosen, C.J., Pessin, J.E., and Judex, S. Adipogenesis is inhibited by brief, daily exposure to high-frequency, extremely low-magnitude mechanical signals. Proc Natl Acad Sci U S A **104**, 17879, 2007.

18. Chung, M.T., Hyun, J.S., Lo, D.D., Montoro, D.T., Hasegawa, M., Levi, B., Januszyk, M., Longaker, M.T., and Wan, D.C. Micro-computed tomography evaluation of human fat grafts in nude mice. Tissue Eng Part C Methods **19**, 227, 2013.

19. Hu, H.H., Nayak, K.S., and Goran, M.I. Assessment of abdominal adipose tissue and organ fat content by magnetic resonance imaging. Obes Rev **12**, e504, 2011.

20. Shen, W., Liu, H., Punyanitya, M., Chen, J., and Heymsfield, S.B. Pediatric obesity phenotyping by magnetic resonance methods. Curr Opin Clin Nutr Metab Care **8**, 595, 2005.

21. Del Vecchio, D.A., and Bucky, L.P. Breast augmentation using preexpansion and autologous fat transplantation: a clinical radiographic study. Plast Reconstr Surg **127**, 2441, 2011.

22. Fiaschetti, V., Pistolese, C.A., Fornari, M., Liberto, V., Cama, V., Gentile, P., Floris, M., Floris, R., Cervelli, V., and Simonetti, G. Magnetic resonance imaging and ultrasound evaluation after breast autologous fat grafting combined with platelet-rich plasma. Plast Reconstr Surg **132**, 498e, 2013.

23. Herold, C., Ueberreiter, K., Busche, M.N., and Vogt, P.M. Autologous fat transplantation: volumetric tools for estimation of volume survival. A systematic review. Aesthetic Plast Surg **37**, 380, 2013.

24. Johnson, D.H., Flask, C.A., Ernsberger, P.R., Wong, W.C., and Wilson, D.L. Reproducible MRI measurement of adipose tissue volumes in genetic and dietary rodent obesity models. J Magn Reson Imaging **28**, 915, 2008.

25. Garcia, M.C., Wernstedt, I., Berndtsson, A., Enge, M., Bell, M., Hultgren, O., Horn, M., Ahren, B., Enerback, S., Ohlsson, C., Wallenius, V., and Jansson, J.O. Mature-onset obesity in interleukin-1 receptor I knockout mice. Diabetes **55**, 1205, 2006.

26. Calderan, L., Marzola, P., Nicolato, E., Fabene, P.F., Milanese, C., Bernardi, P., Giordano, A., Cinti, S., and Sbarbati, A. In vivo phenotyping of the ob/ob mouse by magnetic resonance imaging and 1H-magnetic resonance spectroscopy. Obesity (Silver Spring) **14**, 405, 2006.

27. Torio-Padron, N., Paul, D., von Elverfeldt, D., Stark, G.B., and Huotari, A.M. Resorption rate assessment of adipose tissue-engineered constructs by intravital magnetic resonance imaging. J Plast Reconstr Aesthet Surg **64**, 117, 2011.

28. Xu, J., Chen, Y., Yue, Y., Sun, J., and Cui, L. Reconstruction of epidural fat with engineered adipose tissue from adipose derived stem cells and PLGA in the rabbit dorsal laminectomy model. Biomaterials **33**, 6965, 2012.

29. Machann, J., Horstmann, A., Born, M., Hesse, S., and Hirsch, F.W. Diagnostic imaging in obesity. Best Pract Res Clin Endocrinol Metab **27**, 261, 2013.

30. L'Heureux, N., Pâquet, S., Labbé, R., Germain, L., and Auger, F.A. A completely biological tissue-engineered blood vessel. FASEB J **12**, 47, 1998.

31. Auger, F.A., Remy-Zolghadri, M., Grenier, G., and Germain, L. The self-assembly approach for organ reconstruction by tissue engineering. E biomed **1**, 75, 2000.

32. Vermette, M., Trottier, V., Menard, V., Saint-Pierre, L., Roy, A., and Fradette, J. Production of a new tissue-engineered adipose substitute from human adipose-derived stromal cells. Biomaterials **28**, 2850, 2007.

33. Fortier, G.M., Gauvin, R., Proulx, M., Vallee, M., and Fradette, J. Dynamic culture induces a cell type-dependent response impacting on the thickness of engineered connective tissues. J Tissue Eng Regen Med **7**, 292, 2013.

34. Vallee, M., Cote, J.F., and Fradette, J. Adipose-tissue engineering: taking advantage of the properties of human adipose-derived stem/stromal cells. Pathol Biol (Paris) **57**, 309, 2009.

35. Labbé, B., Marceau Fortier, G., and Fradette, J. Cell sheet technology for tissue engineering: the self-assembly approach using adipose-derived stromal cells. In: Gimble J.M., Bunnell B.A., eds. Adipose-Derived Stem Cells: Methods and Protocols. New York: Humana Press, 2011, pp. 429-41.

36. Hill, A.M., LaForgia, J., Coates, A.M., Buckley, J.D., and Howe, P.R. Estimating abdominal adipose tissue with DXA and anthropometry. Obesity (Silver Spring) **15**, 504, 2007.

37. Clarke, S.E., Weinmann, H.-J., Dai, E., Lucas, A.R., and Rutt, B.K. Comparison of two blood pool contrast agents for 0.5-T MR angiography: experimental study in rabbits. Radiology **214**, 787, 2000.

38. Donahue, K.M., Burstein, D., Manning, W.J., and Gray, M.L. Studies of Gd-DTPA relaxivity and proton exchange rates in tissue. Magn Reson Med **32**, 66, 1994.

39. Gadian, D.G., Payne, J.A., Bryant, D.J., Young, I.R., Carr, D.H., and Bydder, G.M. Gadolinium-DTPA as a contrast agent in MR imaging--theoretical projections and practical observations. J Comput Assist Tomogr **9**, 242, 1985.

40. Sbarbati, A., Guerrini, U., Marzola, P., Asperio, R., and Osculati, F. Chemical shift imaging at 4.7 tesla of brown adipose tissue. J Lipid Res **38**, 343, 1997.

41. Hamilton, G., Smith, D.L., Jr., Bydder, M., Nayak, K.S., and Hu, H.H. MR properties of brown and white adipose tissues. J Magn Reson Imaging **34**, 468, 2011.

42. Hu, H.H., and Kan, H.E. Quantitative proton MR techniques for measuring fat. NMR Biomed **26**, 1609, 2013.

43. Hu, H.H., Smith, D.L., Jr., Nayak, K.S., Goran, M.I., and Nagy, T.R. Identification of brown adipose tissue in mice with fat-water IDEAL-MRI. Journal of magnetic resonance imaging : JMRI **31**, 1195, 2010.

44. Hamilton, G., Yokoo, T., Bydder, M., Cruite, I., Schroeder, M.E., Sirlin, C.B., and Middleton, M.S. In vivo characterization of the liver fat (1)H MR spectrum. NMR Biomed **24**, 784, 2011.

45. Delikatny, E.J., Chawla, S., Leung, D.J., and Poptani, H. MR-visible lipids and the tumor microenvironment. NMR Biomed **24**, 592, 2011.

46. Tanzi, M.C., and Fare, S. Adipose tissue engineering: state of the art, recent advances and innovative approaches. Expert Rev Med Devices **6**, 533, 2009.

47. Bushberg, J.T., Seibert, J.A., Leidholt, E.M., Jr, and Boone, J.M. The essential physics of medical imaging. Second ed. Philadelphia: Lippincott Williams & Wilkins, 2002.

48. Weissleder, R., Cheng, H.C., Marecos, E., Kwong, K., and Bogdanov, A., Jr. Non-invasive in vivo mapping of tumour vascular and interstitial volume fractions. Eur J Cancer **34**, 1448, 1998.

49. Preda, A., Novikov, V., Moglich, M., Turetschek, K., Shames, D.M., Brasch, R.C., Cavagna, F.M., and Roberts, T.P. MRI monitoring of Avastin antiangiogenesis therapy using B22956/1, a new blood pool contrast agent, in an experimental model of human cancer. J Magn Reson Imaging **20**, 865, 2004.

50. Parker, G.J., and Tofts, P.S. Pharmacokinetic analysis of neoplasms using contrast-enhanced dynamic magnetic resonance imaging. Top Magn Reson Imaging **10**, 130, 1999.

51. Qi, X.L., Burns, P., Hong, J., Stainsby, J., and Wright, G. Characterizing blood volume fraction (BVF) in a VX2 tumor. Magn Reson Imaging **26**, 206, 2008.

52. Ivanuša, T., Beravs, K., Medič, J., Serša, I., Serša, G., Jevtič, V., Demsar, F., and Mikac, U. Dynamic contrast enhanced MRI of mouse fibrosarcoma using small-molecular and novel macromolecular contrast agents. Phys Med **23**, 85, 2007.

53. Thornhill, J., and Halvorson, I. Intrascapular brown adipose tissue (IBAT) temperature and blood flow responses following ventromedial hypothalamic stimulation to sham and IBAT-denervated rats. Brain Res **615**, 289, 1993.

54. Astrup, A., Bulow, J., and Madsen, J. Interscapular brown adipose tissue blood flow in the rat. Determination with 133xenon clearance compared to the microsphere method. Pflugers Arch **401**, 414, 1984.

55. Nakayama, A., Bianco, A.C., Zhang, C.Y., Lowell, B.B., and Frangioni, J.V. Quantitation of brown adipose tissue perfusion in transgenic mice using near-infrared fluorescence imaging. Mol Imaging **2**, 37, 2003.

56. Ciucurel, E.C., and Sefton, M.V. Del-1 overexpression in endothelial cells increases vascular density in tissue-engineered implants containing endothelial cells and adipose-derived mesenchymal stromal cells. Tissue Eng Part A **20**, 1235, 2014.

57. Heit, Y.I., Lancerotto, L., Mesteri, I., Ackermann, M., Navarrete, M.F., Nguyen, C.T., Mukundan, S., Jr., Konerding, M.A., Del Vecchio, D.A., and Orgill, D.P. External volume expansion increases subcutaneous thickness, cell proliferation, and vascular remodeling in a murine model. Plast Reconstr Surg **130**, 541, 2012.

58. Choi, Y.D., Shin, H.S., and Mok, J.O. Impaired survival of autologous fat grafts by diabetes mellitus in an animal model: a pilot study. Aesthet Surg J **34**, 168, 2014.

59. Alghoul, M., Mendiola, A., Seth, R., Rubin, B.P., Zins, J.E., Calabro, A., Siemionow, M., and Kusuma, S. The effect of hyaluronan hydrogel on fat graft survival. Aesthet Surg J **32**, 622, 2012.

60. Ma, Z., Han, D., Zhang, P., Yang, J.F., Wang, Y., Zhang, Y., Yang, D., and Liu, J. Utilizing muscle-derived stem cells to enhance long-term retention and aesthetic outcome of autologous fat grafting: pilot study in mice. Aesthetic Plast Surg **36**, 186, 2012.

61. Thanik, V.D., Chang, C.C., Lerman, O.Z., Allen, R.J., Jr., Nguyen, P.D., Saadeh, P.B., Warren, S.M., Levine, J.P., Coleman, S.R., and Hazen, A. A murine model for studying diffusely injected human fat. Plast Reconstr Surg **124**, 74, 2009.

62. Frerich, B., Winter, K., Scheller, K., and Braumann, U.D. Comparison of different fabrication techniques for human adipose tissue engineering in severe combined immunodeficient mice. Artif Organs **36**, 227, 2012.

63. Zhang, M.Y., Ding, S.L., Tang, S.J., Yang, H., Shi, H.F., Shen, X.Z., and Tan, W.Q. Effect of Chitosan Nanospheres Loaded with VEGF on Adipose Tissue Transplantation: A Preliminary Report. Tissue Eng Part A 2014.

64. Hamed, S., Egozi, D., Dawood, H., Keren, A., Kruchevsky, D., Ben-Nun, O., Gilhar, A., Brenner, B., and Ullmann, Y. The chemokine stromal cell-derived factor-1alpha promotes endothelial progenitor cell-mediated neovascularization of human transplanted fat tissue in diabetic immunocompromised mice. Plast Reconstr Surg **132**, 239e, 2013.

Reprint author

Julie Fradette, Ph.D.

Département de chirurgie,

Pavillon Ferdinand-Vandry, Université Laval, Québec, QC, G1V 0A6, Canada.

E-mail address: julie.fradette@chg.ulaval.ca

Telephone: 1-418-990-8255 #1713

Fax: 1-418-990-8248

Table 1. T_1 and T_2 values measured for reconstructed and native tissues.

	Total signal				**peak @ 4.7ppm**				**peak @ 1.3ppm**			
	T_1 (ms)	±	T_2 (ms)	±	T_1 (ms)	±	T_2 (ms)	±	T_1 (ms)	±	T_2 (ms)	±
Reconstructed adipose tissue	**813**	**76**	**118**	**8**	**1107**	**118**	**119**	**10**	**200**	**53**	**108**	**9**
Reconstructed connective tissue	**970**	**107**	**98**	**5**	**970**	**107**	**98**	**5**	***n.a.**	***n.a.**	***n.a.**	***n.a.**
Native human fat	**300**	**n.a.**	**158**	**n.a.**	**1440**	**n.a.**	**146**	**n.a.**	**190**	**n.a.**	**152**	**n.a.**
Native murine fat	**500**	**n.a.**	**213**	**n.a.**	**1400**	**n.a.**	**220**	**n.a.**	**240**	**n.a.**	**200**	**n.a.**

*No clear triglyceride peak was evidenced for the reconstructed connective tissue.

Table 2. Signal enhancement ratios (S_1/S_0) of each measured graft, and corresponding blood volume fraction (f) calculated from Equation S6.

Injection time	Number of grafts	*Signal enhancement ratio* (S_1/S_0)	Corresponding blood fraction (f) based on Equation 6 (*)
14 days	**n = 4**	**1.36 ± 0.05**	**0.078 ± 0.018 (7.8 ± 1.8%)**
21 days	**n = 4**	**1.31 ± 0.07**	**0.062 ± 0.021 (6.2 ± 2.1%)**

*Error was calculated based on the standard deviation range of T_{1g} (the factor having by far the strongest incidence on the results of blood fraction calculated using Equation S6). **mouse weight was set to 23 g +/- 1 g, for an expected concentration of Gd in the blood of 1.4 mM.

Figure Captions

FIG. 1. ^{1}H-NMR spectra (60 MHz) of **(A)** reconstructed adipose tissue, **(B)** reconstructed connective tissue, **(C)** native human fat, and **(D)** native murine fat.

FIG. 2. Appearance of human tissue-engineered adipose tissues according to different reconstruction models. **(A)** Representative appearance upon grafting for substitutes of series 1 and 2. **(B)** Representative images for substitutes of serie 3 upon grafting, **(C)** after histological processing and Masson's trichrome staining of tissue samples at the day of implantation and **(D)** 7 days after implantation. Scale in mm **(A, B, D)**. Scale bar: **(C)** 100 µm.

FIG. 3. T_1-w. spin echo images of reconstructed adipose tissues at **(A)** the day of implantation, **(B)** one, **(C)** three, and **(D)** six weeks after implantation. **(E)** Volume maintenance of reconstructed adipose substitutes calculated from T_1-w. spin echo images up to 6 weeks after implantation. Data are presented as mean ± standard deviation. N = 2 independent grafting experiments. Three series: serie 1 (n = 5), serie 2 (n = 3-6), serie 3 (n = 5-6). Statistical analysis of week to week differences in each serie was performed by one-way ANOVA followed by Tukey's post-hoc test ($p < 0.05$).

FIG. 4. Aspect of reconstructed adipose tissue grafts **(A-D)** three weeks and **(E-H)** six weeks after implantation. Representative images of grafted tissues after 3 weeks **(A, B)** upon harvesting (macroscopic) and **(C)** after histological processing and Masson's trichrome staining. Merging of multiple images allowed the reconstitution of large tissue areas for analysis (m = murine muscle). **(C', C'')** Higher magnification images show regions of the grafted tissue featuring varying degrees of adipocytes (void spaces) as well as an abundant extracellular matrix (in blue). The

presence of blood vessels (arrowheads and boxed area in **C'**) is indicative of graft vascularization. **(D)** represents another area from a different grafted substitute. Similarly, 6 weeks after grafting **(E, F)** macroscopic and **(G-H)** histological images of the grafts reveal a healthy appearance with the persistence of numerous adipocytes shown at higher magnification (boxed areas in **G'**, **G''**). Once again, vessels are present within the grafted tissue (arrowheads and boxed area in **G''**). **(H)** is a representative area from a different grafted substitute. Scale in mm **(A, B, E, F)**. Scale bars: **(C, G)** 500 µm; **(C', C'', D, G', G'', H)** 100 µm; (**C', G''** boxed areas) 10 µm.

FIG. 5. Blood perfusion studies by DCE-MRI: T_1-w. spin echo images **(A)** before injection of the contrast agent; **(B)** after injection (30 min.); S_1/S_0 signal enhancement profiles after injection, measured in reconstructed adipose grafts *in vivo* at **(C)** 14 and **(D)** 21 days after implantation.

Figure 1

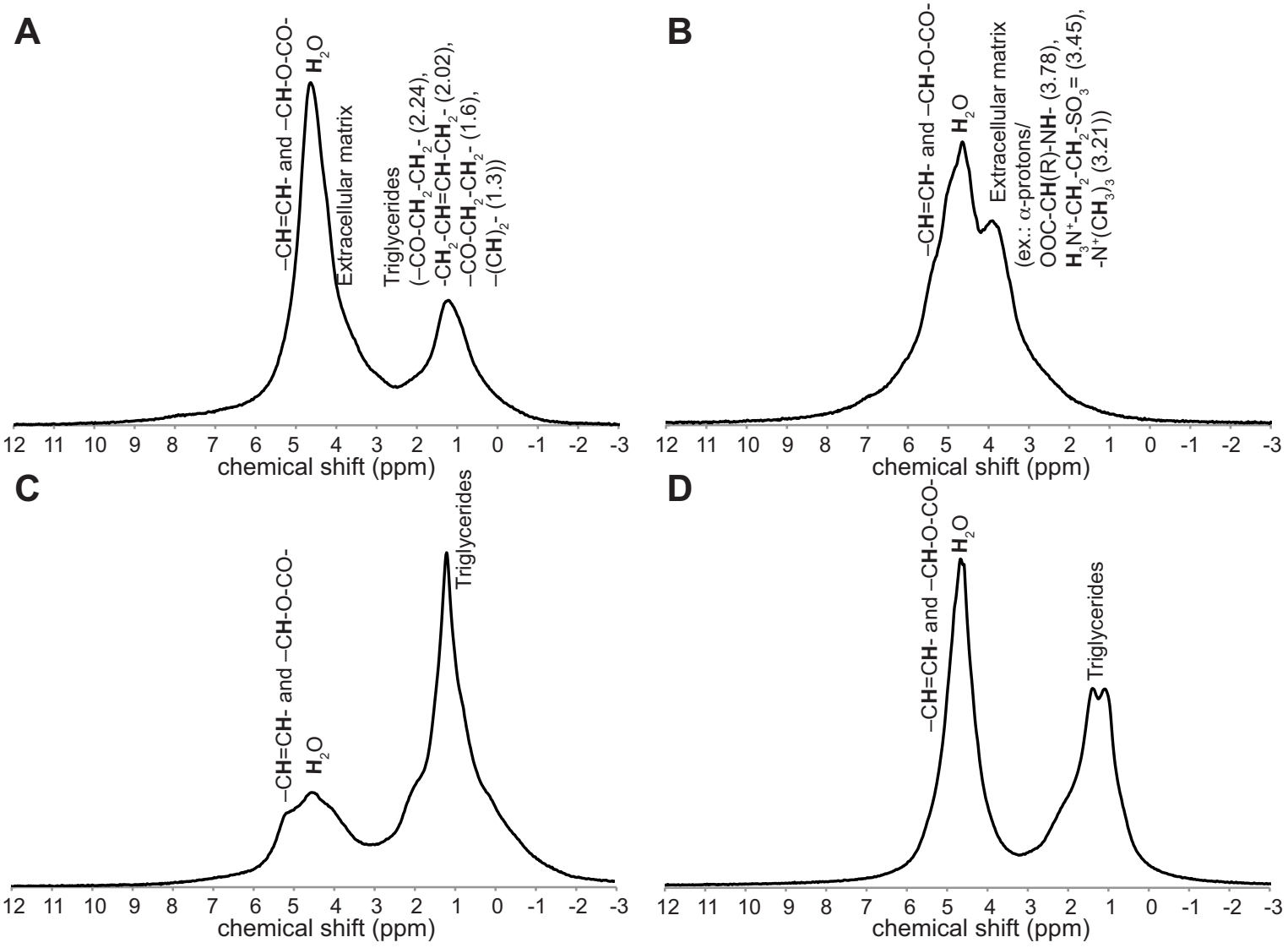
A
–CH=CH- and –CH-O-CO-
H2O
Extracellular matrix
Triglycerides
(–CO-CH2-CH2- (2.24),
-CH2-CH=CH-CH2- (2.02),
–CO-CH2-CH2- (1.6),
–(CH)2- (1.3))
12 11 10 9 8 7 6 5 4 3 2 1 0 -1 -2 -3
chemical shift (ppm)
B
–CH=CH- and –CH-O-CO-
H2O
Extracellular matrix
(ex.: α-protons/
OOC-CH(R)-NH- (3.78),
H3N+-CH2-CH2-SO3= (3.45),
-N+(CH3)3 (3.21))
12 11 10 9 8 7 6 5 4 3 2 1 0 -1 -2 -3
chemical shift (ppm)
C
–CH=CH- and –CH-O-CO-
H2O
Triglycerides
12 11 10 9 8 7 6 5 4 3 2 1 0 -1 -2 -3
chemical shift (ppm)
D
–CH=CH- and –CH-O-CO-
H2O
Triglycerides
12 11 10 9 8 7 6 5 4 3 2 1 0 -1 -2 -3
chemical shift (ppm)

Figure 2

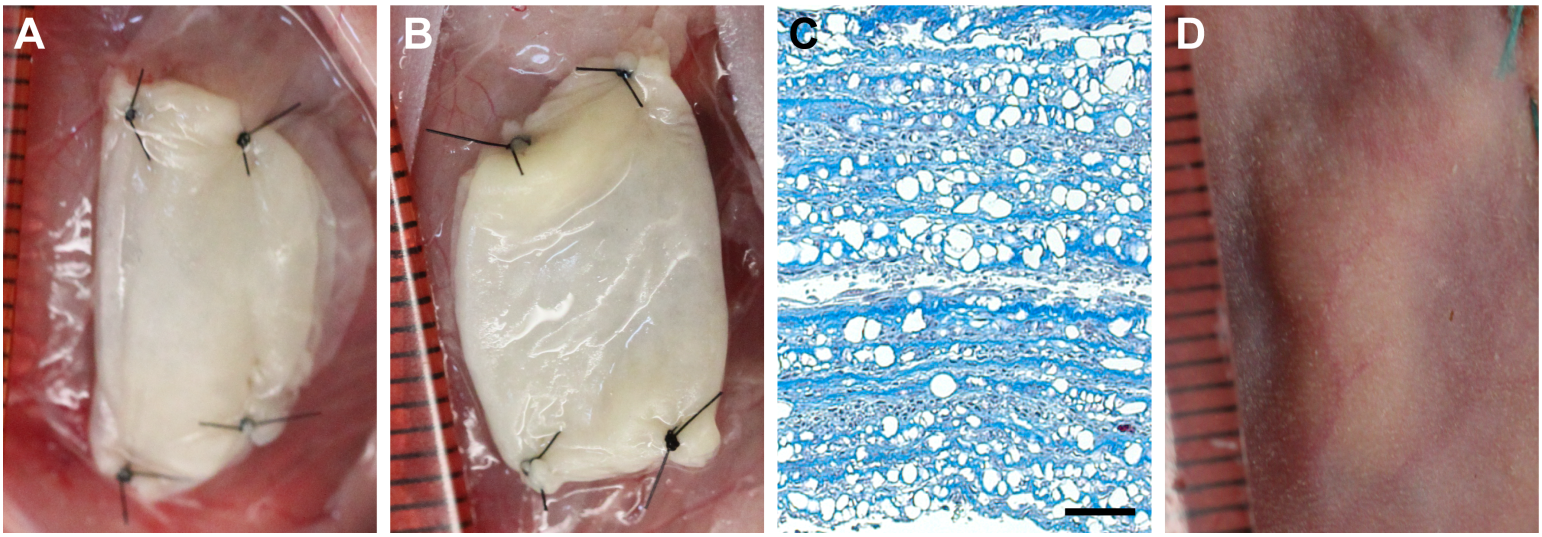

Figure 3

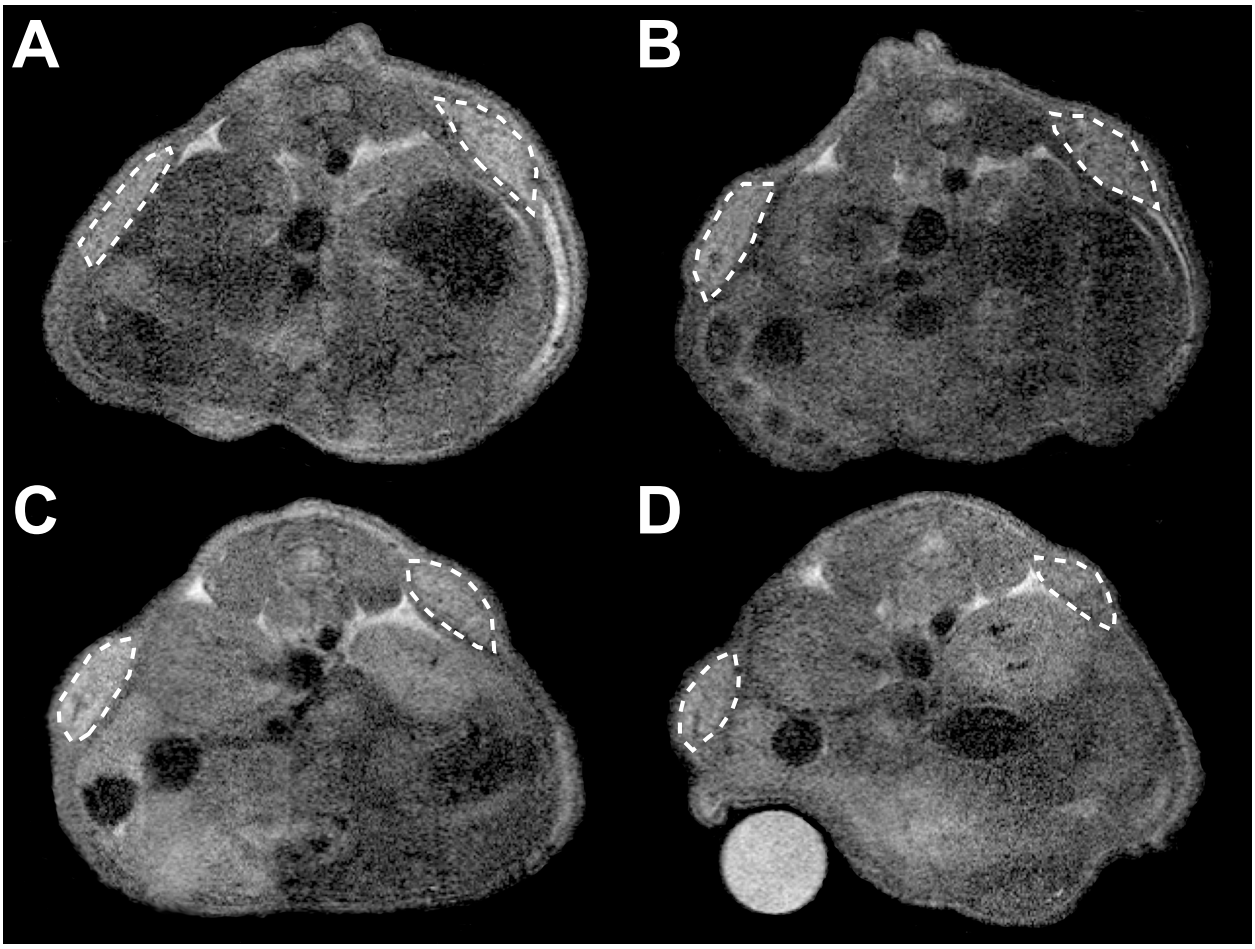
A
B
C
D

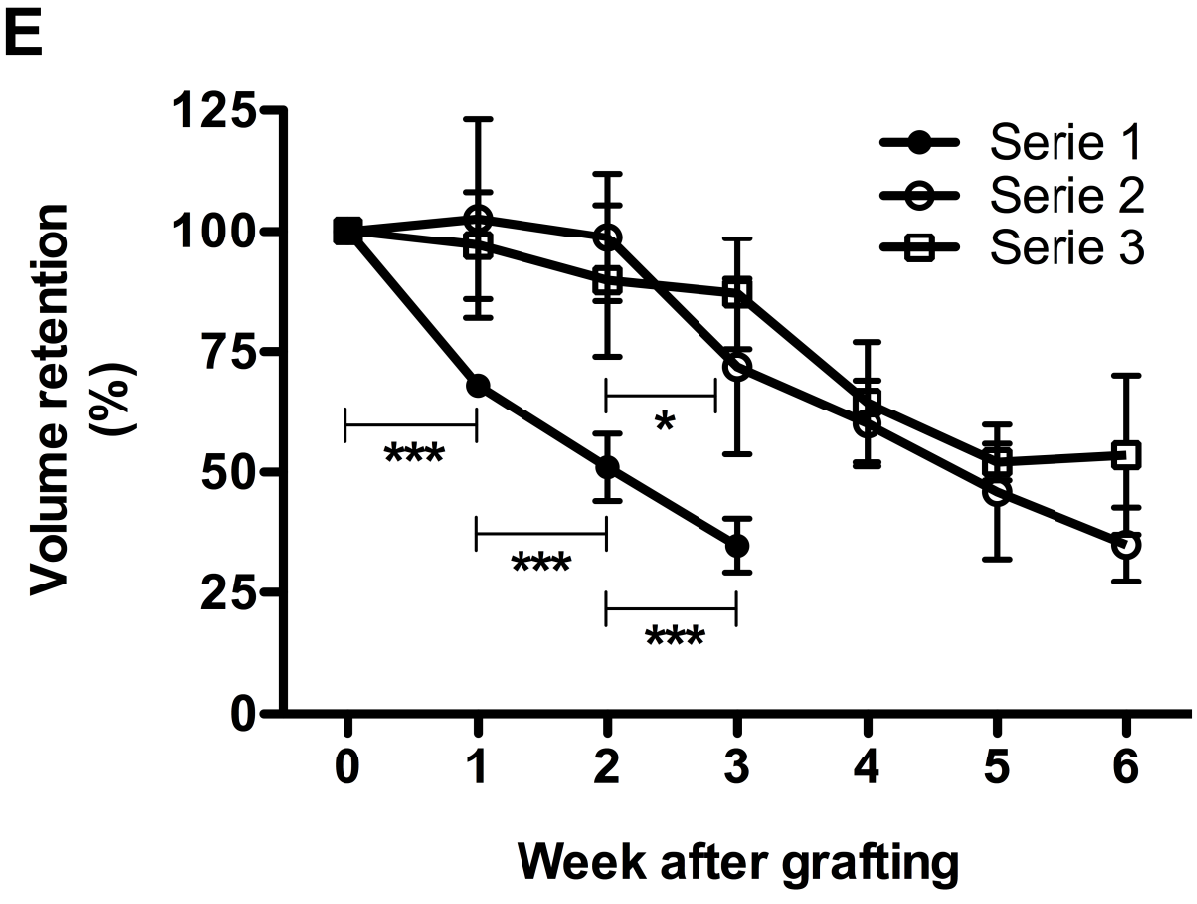
E
125
100
75
50
25
0
Volume retention (%)
0
1
2
3
4
5
6
Week after grafting
Serie 1
Serie 2
Serie 3
***
***
***
*

Figure 4

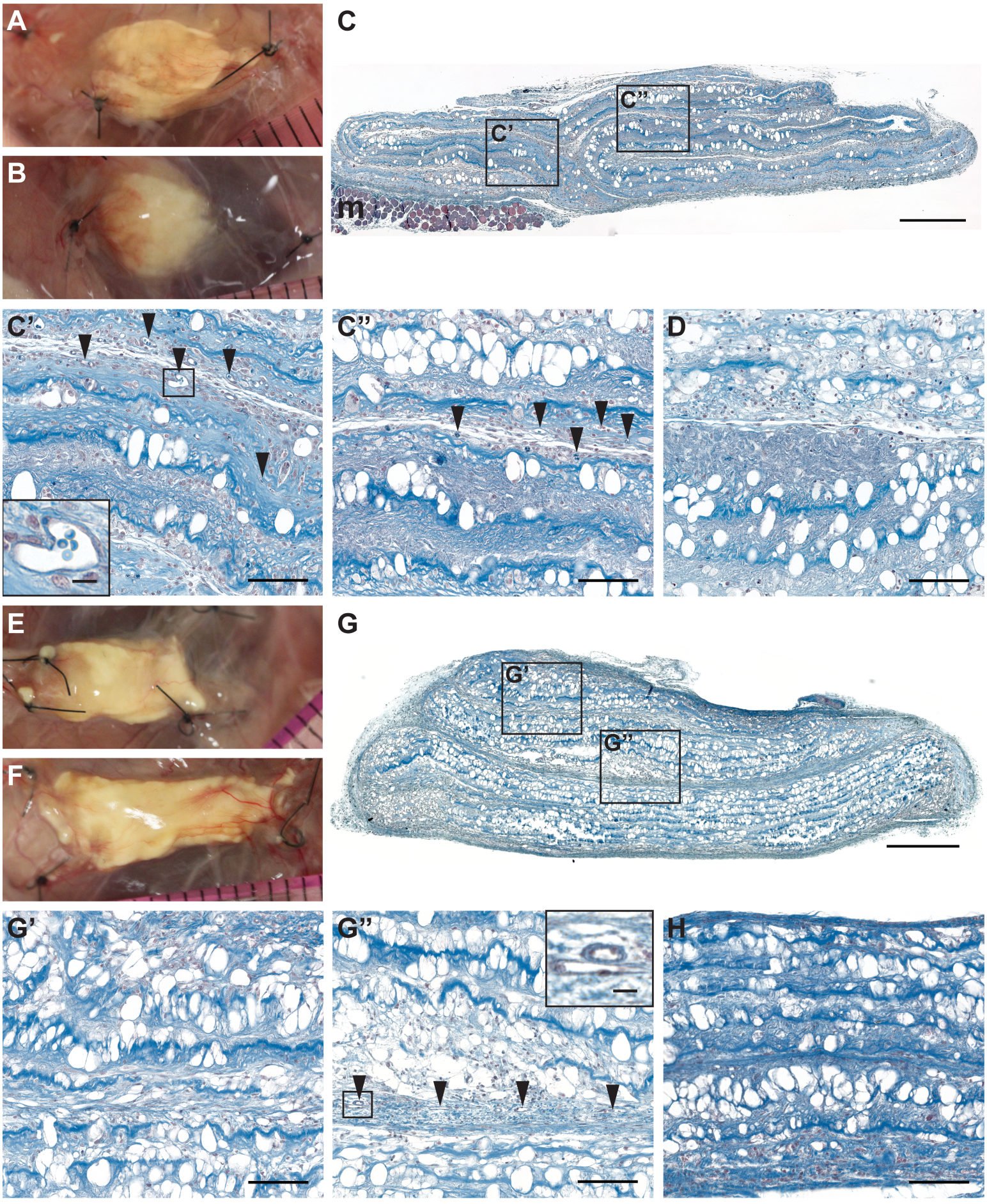

Figure 5

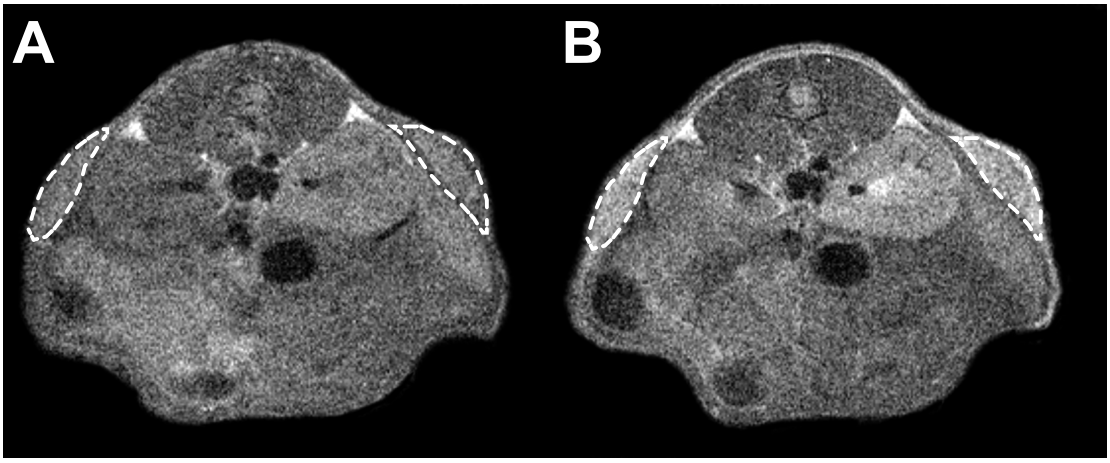
A
B

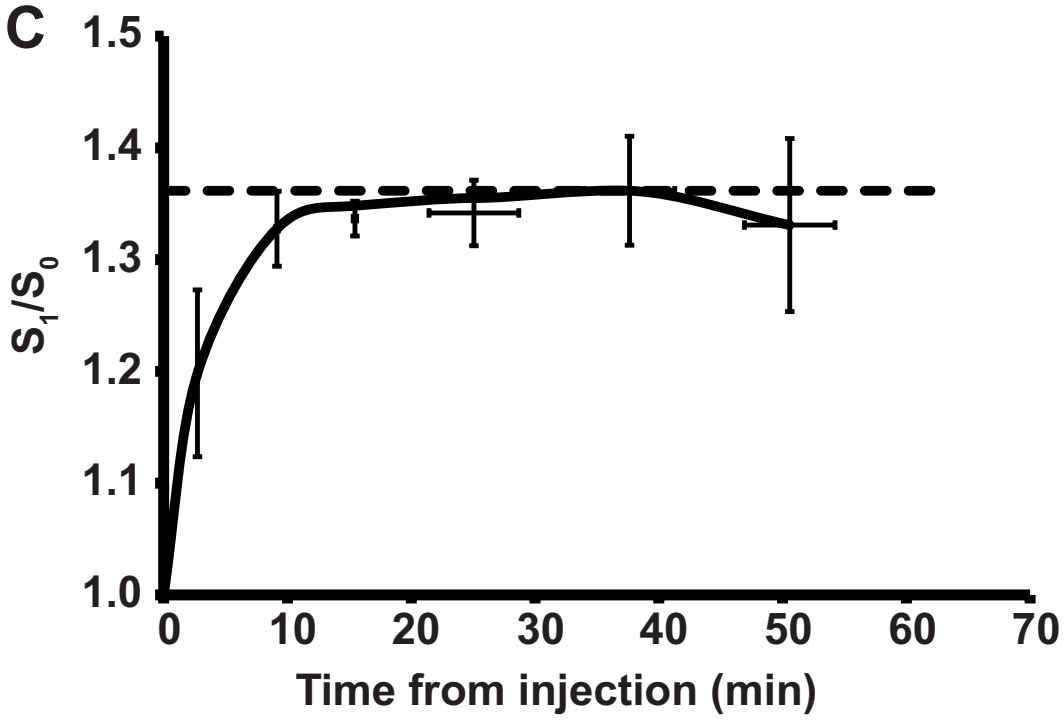
C
1.5
1.4
1.3
1.2
1.1
1.0
S1/S0
0
10
20
30
40
50
60
70
Time from injection (min)

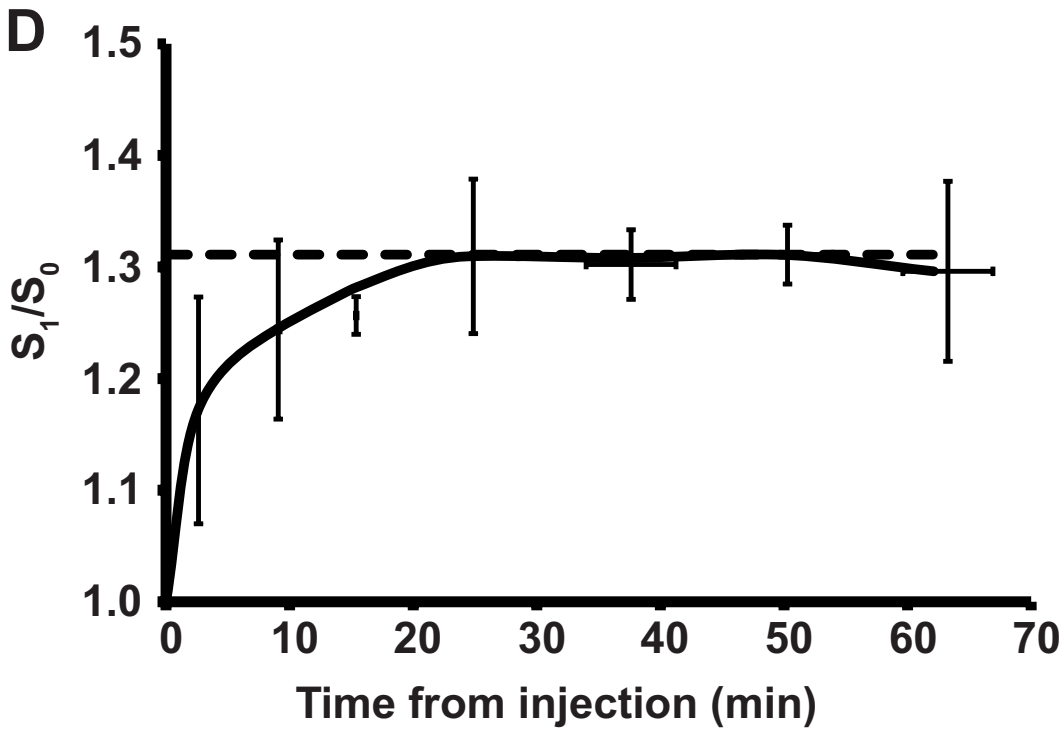
D
1.5
1.4
1.3
1.2
1.1
1.0
S1/S0
0
10
20
30
40
50
60
70
Time from injection (min)

Supplementary Materials and Methods

Vascular volume quantification

The vascular volume in adipose tissue grafts was measured considering that grafts were composed of two different tissues (reconstructed adipose tissue and blood), each one represented with a precise volume fraction per voxel. The relaxation rate of each tissue is the inverse of the relaxation time ($R_{i=1,2} = 1/T_i$) and contributions from a paramagnetic agent are taken into account by the following relationship:

$$R_{i=1,2} = \frac{1}{T_{id}} + r_i[Gd] \qquad \text{Equation 1}$$

Where $T_{i,d}$ is the relaxation time of the matrix (water, or organic tissue), r_i is the relaxivity (r_1= longitudinal relaxivity and r_2= transverse relaxivity) and [Gd] is the local paramagnetic ion concentration. Then, considering a model of two tissues, in which R_{ig} is the relaxation rate of the adipose tissue graft (without blood), R_{ib} is the relaxation rate of Gd-containing blood, and R_{iv} is the total relaxation rate measured in the vascularized adipose tissue graft, the following equations were assumed, with f as the total blood volume fraction in the graft:

$$R_{i(=1,2)g} = \frac{1}{T_{ig}} \qquad \text{Equation 2}$$

Where T_{1g} and T_{2g} are the graft relaxation times measured *in vitro* with NMR (for [Gd] = 0);

$$R_{i(=1,2)b} = \frac{1}{T_{ib}} + r_i[Gd] \qquad \text{Equation 3}$$

Where T_{1b} and T_{2b} are the mouse blood relaxation times at 1 T (with [Gd] = 0). The relaxivities of Gadomer 17 at 1 T and 37°C were taken as $r_1 = 12\ mM^{-1}s^{-1}$ and $r_2 = 14.4\ mM^{-1}s^{-1}$.[1] We made the reasonable assumption that all Gd was contained in the blood pool in the first 30 minutes [2] following injection, resulting in 1.61 mM Gd just after *i.v.* injection (80 ml blood/kg mouse body weight).[3] Therefore, the expression for the total relaxation rate in a vascularized graft is given as:

Equation 4

Then, the equation of signal from spin-echo sequences is given by:

$$S_0 = \rho(1 - e^{-TR/T_1})(e^{-TE/T_2}) \qquad \text{Equation 5}$$

Where TR is the repetition time, TE echo time, and r is the proton density. Considering $R_{iv(Gd=0)}$, and $R_{iv(Gd)}$ being the relaxation rates of the vascularized tissues before and after injection of Gd, respectively, the signal enhancement ratio following contrast media injections, is quantified as follows:

$$\frac{S_1}{S_0} = \frac{(1 - e^{(-TR/T_{1v(Gd)})})(e^{-TE/T_{2v(Gd)}})}{(1 - e^{(-TR/T_{1v(Gd=0)})})(e^{-TE/T2v(Gd=0)})} = \frac{(1 - e^{(-TR \cdot R_{1v(Gd)})})(e^{-TE \cdot R_{2v(Gd)}})}{(1 - e^{(-TR \cdot R_{1v(Gd=0)})})(e^{-TE \cdot R_{2v(Gd=0)}})} \qquad \text{Equation 6}$$

Therefore, the relative blood fraction (f) is extracted using equations 4 and 6, as well as with experimental S_1/S_0 values measured by DCE-MRI (ROIs drawn over each graft).

Supplementary References

1. Nicolle, G., Tóth, É., Eisenwiener, K.-P., Mäcke, H., and Merbach, A. From monomers to micelles: investigation of the parameters influencing proton relaxivity. J Biol Inorg Chem **7**, 757, 2002.

2. Wen, X., Jackson, E.F., Price, R.E., Kim, E.E., Wu, Q., Wallace, S., Charnsangavej, C., Gelovani, J.G., and Li, C. Synthesis and characterization of poly(L-glutamic acid) gadolinium chelate: a new biodegradable MRI contrast agent. Bioconjug Chem **15**, 1408, 2004.

3. Barbee, R.W., Perry, B.D., Re, R.N., and Murgo, J.P. Microsphere and dilution techniques for the determination of blood flows and volumes in conscious mice. Am J Physiol **263**, R728, 1992.

SUPPLEMENTARY FIG. S1. T_1-w spin echo images of grafts at the day of implantation: **(A)** reconstructed adipose tissue (left arrow) and reconstructed connective tissue (right arrow); **(B)** murine fat graft (left arrow) and human fat graft (right arrow). A 4.5-mm diameter triglyceride bead was placed next to the left side graft for faster positioning.

SUPPLEMENTARY FIG. S2. Human fat graft (left arrow) and reconstructed adipose tissue (right arrow) at the day of implantation, imaged with **(A)** T_1-w imaging and **(B)** STIR. Arrowheads: endogenous fat of the subcutaneous layer.

SUPPLEMENTARY FIG. S3. Volume correlation between weight measurements and MRI measurements of reconstructed adipose tissue grafts using Spearman's rank correlation coefficient and r^2 coefficient of determination. (N = 2 experiments, n = 12 grafts).

Supplementary Figure S1

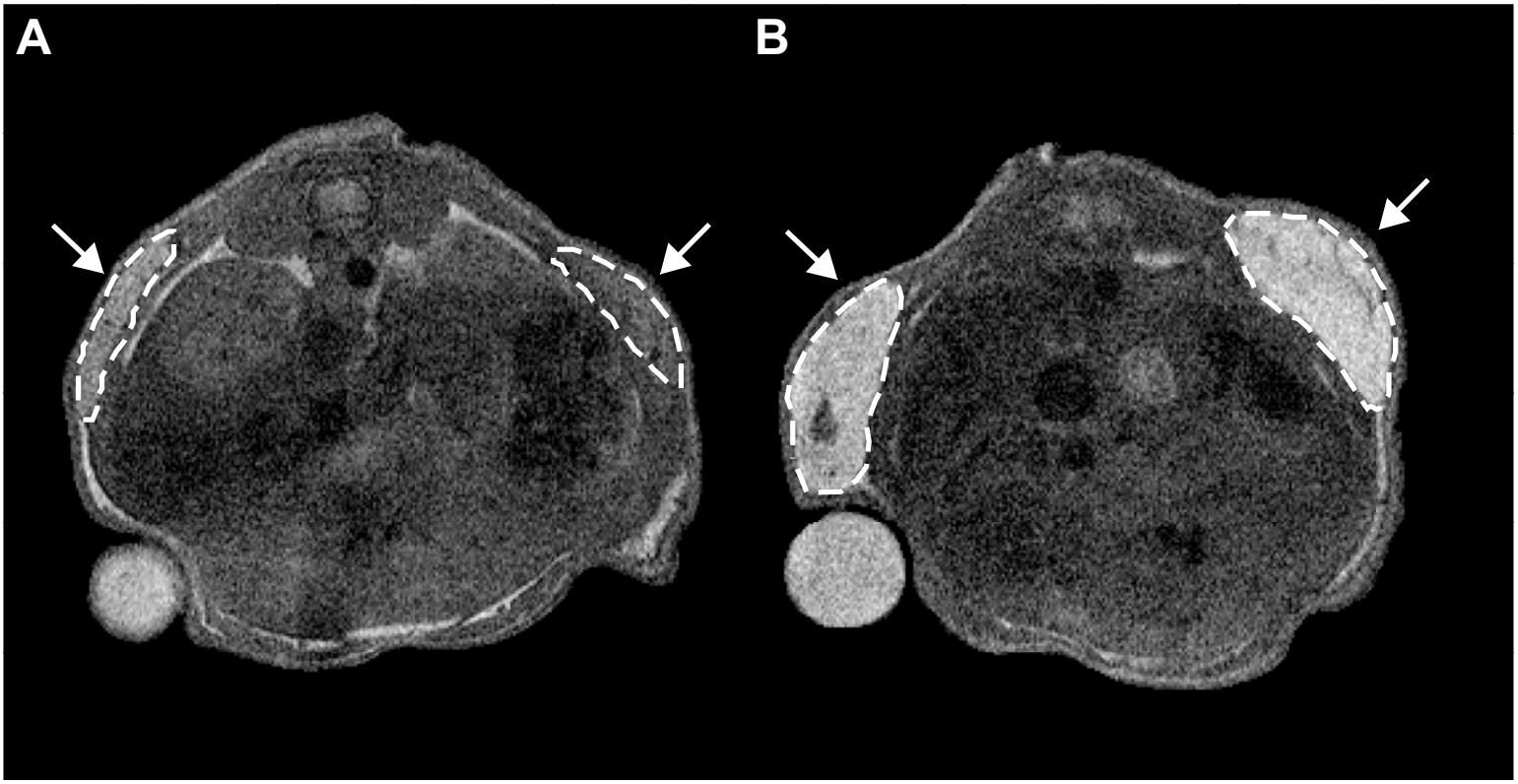

Supplementary Figure S2

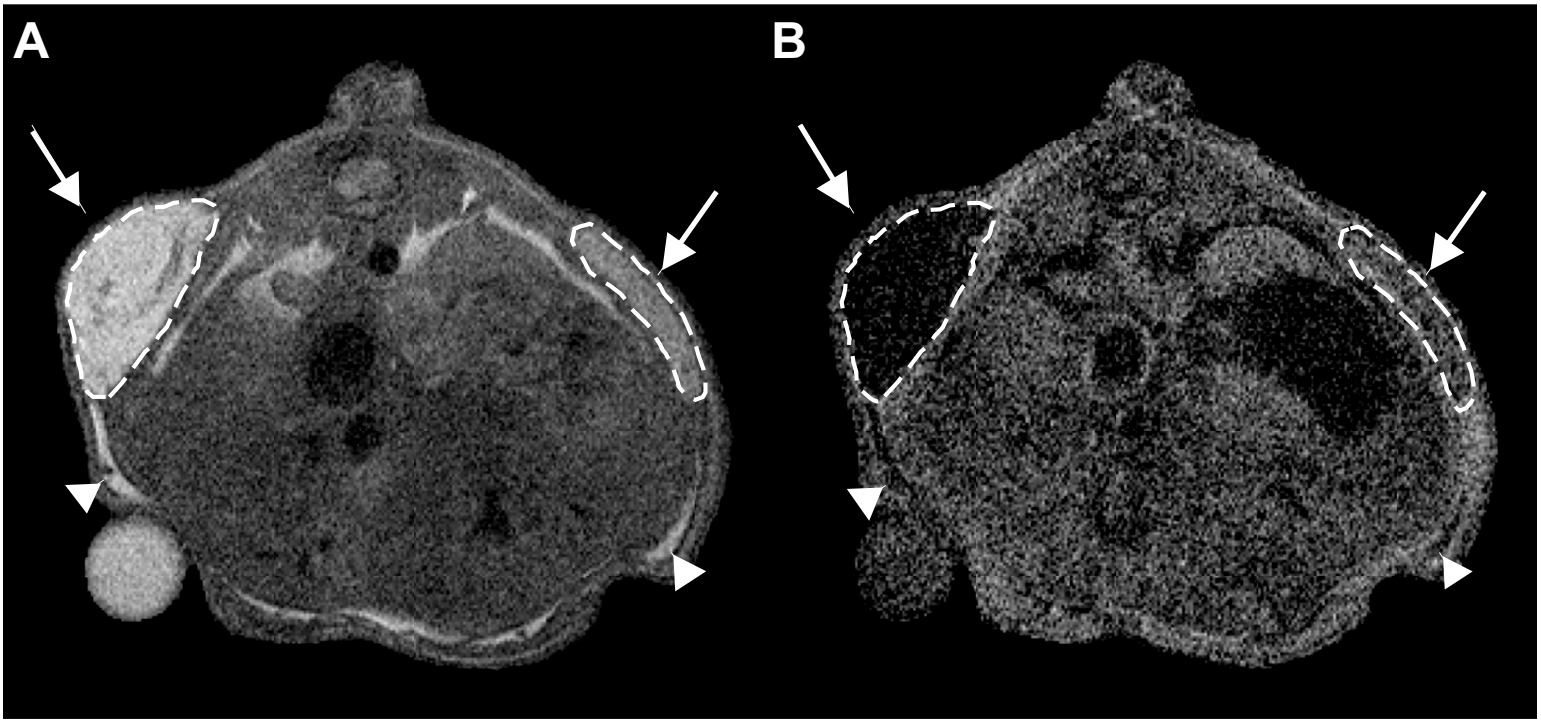

Supplementary Figure S3